GEOFIZIKA VOL. 43 2026

DOI: https://doi.org/10.15233/gfz.2026.43.6
Original scientific paper

Planetary-scale sea-level variability in the Adriatic Sea under present and future climate conditions

Iva Međugorac[1,2,3]* *and Ivan Güttler*[4]

[1] University of Nova Gorica, Vipavska 13, SI-5000 Nova Gorica, Slovenia

[2] Slovenian Environment Agency, Vojkova 1b, 1000 Ljubljana, Slovenia

[3] Department of Geophysics, Faculty of Science, University of Zagreb, Horvatovac 95, 10000, Zagreb, Croatia

[4] Croatian Meteorological and Hydrological Service, Ravnice 48, 10000 Zagreb, Croatia

Received 26 November 2025, in final form 7 March 2026

Sea-level variability on planetary time scales (10–100 d) is a prominent feature of the Adriatic Sea and an important preconditioner of coastal flooding. We characterized its properties in the present climate using the nearly century-long Bakar tide-gauge record (1929–2021) and mean sea-level pressure from ERA5 reanalysis, and assessed projected changes using three regional climate model simulations (ALADIN, CCLM, and RACMO). High coherence between sea level and mean sea-level pressure in the 10–100 d band justified using mean sea-level pressure as a proxy for planetary-scale sea level in future climate. Extreme planetary-scale episodes were defined as sea-level anomalies $\geq +19$ cm (98th percentile of Bakar sea level filtered at 10–100 d) and mean sea-level pressure ≤ -13.5 hPa, separated by at least ten days. In the past period, extreme sea-level episodes peaked in the cold season, occurred typically once or twice per year, lasted three to six days, and showed no significant century-scale trend in intensity, frequency, or duration. Evaluation of regional climate models for the period 1971–2000 showed that all models reproduced the observed seasonal cycle and episode intensity, while the CCLM and especially RACMO models tended to overestimate frequency and duration. Future projections (2039–2068, 2069–2098) under RCP4.5 and RCP8.5 indicated no robust changes in episode intensity, frequency or duration suggesting that planetary-scale atmospheric forcing over the northern Adriatic is unlikely to change substantially in warmer climates. Consequently, future flood risk will be governed primarily by mean sea-level rise and its superposition with tides and storm surges, rather than by strengthened planetary-scale anomalies.

Keywords: Adriatic Sea, sea level, mean sea-level pressure, planetary-scale component, regional climate models, RCP4.5, RCP8.5

1. Introduction

Sea-level (SL) variability on timescales of 10–100 d – often referred to in the literature as the *planetary-scale variability / component* – is a prominent feature of the Adriatic Sea (Fig. 1) (e.g., Pasarić and Orlić, 2001; Međugorac et al., 2025). Up to 30% of the Adriatic's SL variance occurs at these periods (Pasarić and Orlić, 2001), largely driven by slowly varying mean sea-level pressure (MSLP) patterns and associated winds (W10). Studies in the Adriatic and wider Mediterranean (e.g., Palumbo and Mazzarella, 1982; Tsimplis and Vlahakis, 1994; Pasarić et al., 2000) have shown that MSLP-SL coherence is very high at periods above 10 d (~0.1 cpd), with SL fluctuations often exceeding the isostatic response (up to –1.7 cm/hPa). This translates into oscillations of several tens of centimeters, with SL variations reaching up to 70 cm in the northern Adriatic (Pasarić and Orlić, 1992).

Changes in MSLP and W10 on 10–100 d timescales are usually linked to the passage of planetary Rossby waves over the Mediterranean (Penzar et al., 1980; Orlić, 1983; Pasarić and Orlić, 1992; Pasarić et al., 2000). Their activity is most pronounced during the cold part of the year, when they are visible as waveforms in the 500-hPa geopotential height (Z500) field, with wavelengths of 6000–8000 km, generally propagating eastward with maximum speeds of ~8 m/s, though they can also be stationary or retrograde. Under barotropic conditions, common in winter, these mid-tropospheric disturbances are reflected at the surface and become evident in MSLP and W10, thereby inducing corresponding SL variability. This relationship holds statistically (Pasarić, 2000), but may not apply in individual cases when the atmosphere is baroclinic or when other low-frequency processes, such as thermohaline variability, influence the *planetary-scale component* – as shown for certain extreme SL events at the Bakar station (Međugorac et al., 2025).

The *planetary-scale component* is important because it preconditions extreme coastal events (e.g., Pasarić and Orlić, 2001; Ferrarin et al., 2021; Ferrarin et al., 2022). It modulates the baseline SL on which shorter-term processes – high-frequency oscillations ($T < \sim 10$ h), tides ($T \sim 12$ and ~24 h), storm surges (~ 10 h $< T < 10$ d), and seiches – are superimposed. Many of the most severe Adriatic flood events have occurred when a long-lasting low-pressure system had already elevated SL, allowing subsequent storm surges and tides to breach flood thresholds more easily (Međugorac et al., 2025). For example, the extreme events of 24 December 1958, 1 December 2012, and 8 December 2020 were all preconditioned by baseline SL anomalies exceeding 25 cm. Statistical analysis of the Adriatic's SL (Šepić et al., 2022) confirmed that the largest positive extremes typically result from multi-scale superposition: a synoptic-scale component coinciding with high tide, superimposed on a raised baseline due to *planetary-scale variability*.

SL processes in the Adriatic, at different temporal and spatial scales, are largely independent due to their relatively small amplitudes compared to the basin depth, which makes nonlinear interactions negligible. This independence

between the dominant components – tides and storm surges, and tides and seiches – has been confirmed through empirical studies (Cerovečki et al., 1997; Marcos et al., 2009) and numerical experiments (Lionello et al., 2005). Owing to this linearity, distinct SL processes, including *planetary-scale variability*, can be isolated using band-pass filtering with appropriate cut-off frequencies and analysed separately.

Characterizing the properties of this SL variability, its frequencies, durations, and amplitudes, is crucial not only for understanding present climate conditions but also for assessing future changes. While mean sea-level rise will undoubtedly increase flood risk (e.g., Weisse et al., 2014; Vitousek et al., 2017; Taherkhani et al., 2020), shifts in atmospheric circulation may also alter the frequency or intensity of prolonged intervals of raised or lowered SL. Recent work has shown that the characteristics of wind forcing at synoptic scales (storm surges) are not expected to change substantially under future scenarios (RCP4.5 and RCP8.5) by the end of the century (Međugorac et al., 2021). However, the future behavior of planetary-scale forcing remains uncertain. Determining whether planetary-scale oscillations will become more frequent, longer-lasting, or more intense is therefore vital, as this directly affects the likelihood of compound flood events in a changing climate.

This study examines how the characteristics of the *planetary-scale component* may evolve under future climate scenarios. In this paper we apply a three-member set of atmosphere-only regional climate models' (RCM) simulations and MSLP fields are used as a proxy to estimate future low-frequency SL variability. Understanding the properties of the *planetary-scale component* is thus a vital step toward projecting future coastal flood risk in the Adriatic region.

The paper is organized as follows: after the Introduction (Section 1), Section 2 describes the data and methods. Section 3 presents the link between SL and MSLP, while Section 4 provides an overview of the characteristics of extreme low-frequency SL episodes in the past period. Section 5 evaluates the regional climate models, while Section 6 compares extreme-event characteristics in future and historical climates and discusses key methodological choices. Finally, Section 7 summarizes the main conclusions.

2. Sea-level and air-pressure data and methods

The datasets used in this study are summarised in Table 1. Hourly SL measurements were obtained from the tide-gauge station at Bakar (TG Bakar), located in the northeastern Adriatic (Fig. 1). This record represents the longest continuous series of a single oceanographic parameter in Croatia. The data are publicly available through the SEANOE database under a CC-BY-NC license. The record spans December 1929 to December 2021 (Međugorac et al., 2022; Međugorac et al., 2024), with one major gap of approximately ten years during

the Second World War and several shorter gaps (lasting up to a few months) prior to 1984 (Međugorac et al., 2022, their Fig. 6). SL values are expressed relative to the mean sea level calculated over the 18.6-year nodal cycle centered on 1971.5 (1962–1980), based on the HVRS71 National Geodetic System (Rožić, 2009). The selection of a single tide-gauge site as representative of the northern Adriatic was considered justified because planetary-scale processes occur at a large spatial scale, such that one station was sufficient. Šepić et al. (2022) demonstrated that SL variability with periods longer than 10 d behaves quasi-uniformly across the entire Adriatic basin (their Figs. 10 and 11), supporting this assumption.

For atmospheric data, two types of MSLP fields were considered over the domain shown in Fig. 1: reanalysis and climate simulations. The reanalysis dataset consists of hourly values from the ERA5 Global Reanalysis (Hersbach et al., 2020), provided on a 0.25° × 0.25° grid (~30 km over the Adriatic). These spatial fields are publicly available from the Copernicus Marine Service Repository (Table 1; Hersbach et al., 2023).

Climate simulations from the Med-CORDEX (Ruti et al., 2016; Somot et al., 2018) and EURO-CORDEX (Jacob et al., 2014) initiatives were also used. Daily outputs from the ALADIN, CCLM, and RACMO regional climate models on a 0.44° × 0.44° grid (~50 km over the Adriatic) were selected. The selection of the models was governed by the conditions to use different GCM boundary conditions in each RCM run, the availability of two RCP scenarios and availability of daily MSLP fields at the time the study was conducted. All spatial fields are publicly available through the CDS and ESGF archives (Table 1).

For climate simulations, three-time intervals were considered: historical (1971–2000), near future (2039–2068), and far future (2069–2098). Two climate scenarios were analysed: RCP4.5 and RCP8.5. The use of RCP scenarios was driven by data availability: the regional climate model simulations employed here were produced within the Med-CORDEX and EURO-CORDEX frameworks based on the CMIP5 experimental design. At the time of the study, CORDEX-CMIP6 simulations over the Mediterranean with daily MSLP fields were not yet available for the required GCM–RCM combinations, as the CORDEX-CMIP6 downscaling effort remains in progress (Katragkou et al., 2024). Importantly, RCP4.5 and SSP2-4.5 target the same nominal end-of-century radiative forcing (~4.5 W/m²), as do RCP8.5 and SSP5-8.5 (~8.5 W/m²) (O'Neill et al., 2016; Riahi et al., 2017). While the socioeconomic narratives and individual greenhouse gas trajectories differ between the frameworks, the resulting radiative forcing pathways are broadly comparable. Since *planetary-scale variability* (10–100 d) is governed by large-scale atmospheric dynamics rather than by the specific greenhouse gas mix, results under RCP4.5 and RCP8.5 can be considered representative of those expected under SSP2-4.5 and SSP5-8.5. The two scenarios bracket a wide range of plausible futures – from intermediate stabilisation to high-end forcing – following established practice in CORDEX-based Adriatic studies (e.g.,

Table 1. The first column lists the data used in this study: measured SL, MSLP from reanalysis (ERA5), and climate simulations (GCM–RCM chain). Temporal (Δt) and spatial (Δx) resolutions are provided in columns 2 and 3, respectively. Data availability is shown in columns 4 and 5. The data sources and the relevant literature describing each dataset are provided in the final column.

Dataset	Δt (h)	Δx (km)	Measurements / Reanalysis / Historical	Projections (RCP4.5 / RCP8.5)	Source and Literature
Sea level	1		12/1929–12/2021		SEANOE, https://doi.org/10.17882/85171, Međugorac et al. (2022)
ERA5	1	~30	1940–		CDS (ERA5-single levels), https://doi.org/10.24381/cds.adbb2d4, Hersbach et al. (2020)
ALADIN GCM: CNRM-CERFACS-CNRM-CM5 RCM: CNRM-ALADIN52	24	~50	1950–2001	2006-2100	CDS (CORDEX-single levels), https://doi.org/10.24381/cds.bc91edc3, Ruti et al. (2016), Somot et al. (2018)
CCLM GCM: MPI-M-MPI-ESM-LR RCM: CCLM-CCLM4-8-18	24	~50	1949–2005	2006-2100	CDS (CORDEX-single levels), https://doi.org/10.24381/cds.bc91edc3, Ruti et al. (2016), Somot et al. (2018)
RACMO GCM: MOHC-HadGEM2-ES RCM: KNMI-RACMO22E	24	~50	1950–2005	2006-11/2099 (RCP4.5) 2006-2099 (RCP8.5)	ESGF database, https://esgf-data.dkrz.de, Jacob et al. (2014)

Međugorac et al., 2021). Finally, domain-averaged MSLP series from both the reanalysis and the climate simulation were obtained by averaging daily fields over the domain shown in Fig. 1.

The main terms used in this study are defined as follows. *Planetary-scale component* was defined as the band-pass filtered SL series (lpSL), obtained using a Kaiser window with half-power cut-off periods at 10 and 100 d. To apply filtering, gaps in the SL data were first filled using linear interpolation. After filtering, the interpolated segments were removed from both the filtered and original series. Only seven data gaps equal to or longer than five days, which could impact *planetary-scale component*, were identified, all occurring before 1984: in 1934, 1936, 1939–1949, 1959, 1980, and 1983. *Planetary-scale component* near these gaps may be affected by edge effects; however, no detected extremes were located within 10 d of these gaps, which may or may not reflect the influence of the filtering process. The MSLP series (which were gap-free) was filtered in the

same way to provide the corresponding atmospheric forcing in this frequency band (lpMSLP). Coherence ($C_{xy}(f)$; unitless) was calculated (Eq. 1, Fig. 2) using Welch's method (Welch, 1967), as the cross power spectral density between MSLP and SL ($P_{xy}(f)$), divided by the product of their individual power spectral densities ($P_{xx}(f)$ for MSLP and $P_{yy}(f)$ for SL):

$$C_{xy}(f) = \frac{\left|P_{xy}(f)\right|^2}{P_{xx}(f)P_{yy}(f)} \tag{1}$$

The calculation was implemented using scipy.signal.coherence function from the Python SciPy library with default parameters (SciPy documentation, 2026). In this function, Pxy(f) is computed as the product of the complex conjugate of the Fast Fourier Transform (FFT) of MSLP and the FFT of SL.

Episodes of extreme high planetary-scale variability (HIGH-lpSL) were defined as time intervals during which lpSL exceeded a predefined threshold (as illustrated in an example in Fig. 3). Consecutive values above the threshold were considered part of the same episode. To ensure independence between events, a minimum separation of ten days was enforced. For example, if lpSL briefly dipped below the threshold between two exceedances occurring within a ten-day window, only the highest peak was retained, and others within ±10 days were excluded. The threshold for HIGH-lpSL was set at +19 cm, corresponding to approximately the 98th percentile of lpSL calculated at TG Bakar over the period 1929–2021. This choice aimed to isolate the most intense anomalies while maintaining a sufficient sample size for robust statistical analysis. Corresponding episodes of extreme low lpMSLP (LOW-lpMSLP) were defined as periods when lpMSLP fell below -13.5 hPa. This threshold was derived from the empirical lpSL–lpMSLP relationship (Fig. 2), ensuring consistency between lpSL extremes and their atmospheric forcing. Both thresholds were selected based on data characteristics at TG Bakar. Figure 3b shows extreme lpSL and lpMSLP episodes (filled areas) during the northern Adriatic flood of December 2020. For most of the period shown, the lpSL series mirrored the lpMSLP series, and both exceeded their respective thresholds during the extreme event on 8 December 2020.

The characteristics of episodes examined in this study were their intensity, frequency and duration. Intensity was defined as the maximum (cm) or minimum (hPa) value reached during the episode (see Fig. 3b). Frequency (events per year) was defined as the number of episodes occurring within a given year. Duration (days) was defined as the length of time during which the variable remained above or below the chosen threshold.

Model performance was evaluated using two statistical tests. Differences in the seasonal distribution of episode onsets (DJF, MAM, JJA, SON) between ERA5 and the RCMs were assessed using a chi-square test (Wilks, 2019) applied to a 2×4 contingency table of seasonal onset counts. The null hypothesis states that both datasets share identical seasonal onset proportions. Differences in the

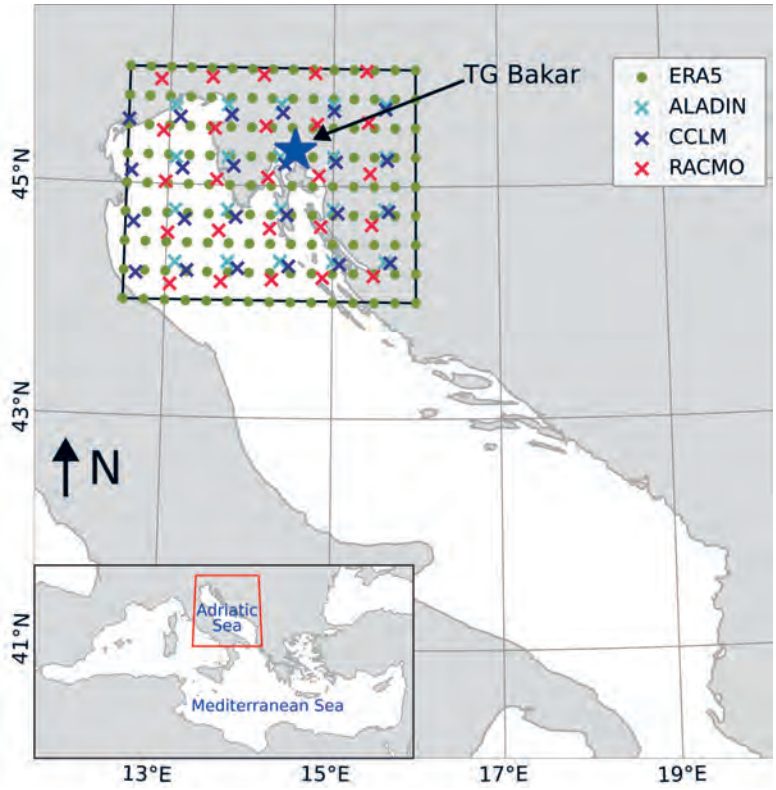


Figure 1. Map of the Adriatic Sea showing the location of the TG Bakar (blue star). The area used for averaging MSLP is indicated by a rectangle. Grids of MSLP series, coming from different sources and at different spatial resolution, are indicated with different markers / colors. The inset in the lower-left corner shows the position of the Adriatic Sea within the Mediterranean Sea.

distributions of episode intensity, frequency, and duration were evaluated using the two-sample Kolmogorov–Smirnov test (Wilks, 2019), which compares empirical cumulative distribution functions to determine whether two samples originate from the same underlying distribution. In both tests, episode onsets were treated as statistically independent, as individual episodes were separated by more than 10 days. Results were considered statistically significant at the 95% confidence level ($\alpha = 0.05$).

3. Coherence between sea level and mean sea-level pressure

Figure 2 shows the coherence between SL and MSLP in the northern Adriatic, calculated separately for the four seasons. Across all seasons, high coherence values are observed at periods longer than about two days, indicating a strong and consistent relationship between SL and MSLP at synoptic to planetary time

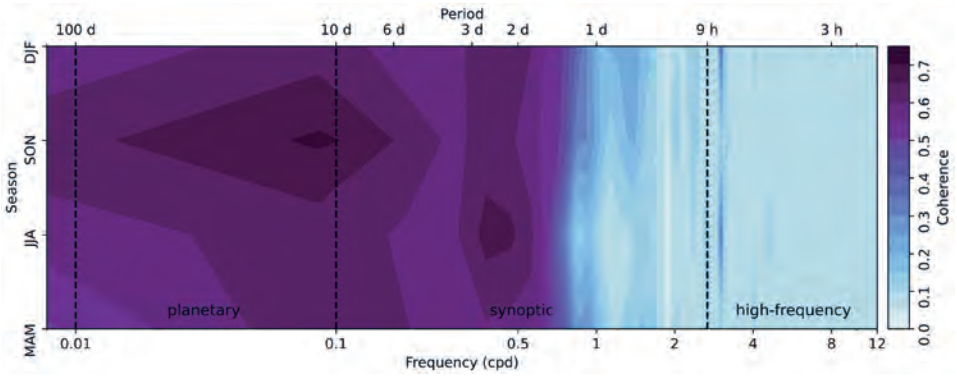


Figure 2. Coherence between hourly SLs at TG Bakar and hourly ERA5 MSLPs averaged over the area shown in Fig. 1 (black rectangle). The abscissa is linearly scaled up to 0.1 cpd, then logarithmically beyond (due to better visibility of low-frequency processes). Vertical lines mark (left to right) periods of 100 d, 10 d, and 9 h – boundaries between long-term, planetary-scale, synoptic and high-frequency processes (e.g., Međugorac et al., 2025). Coherence is shown for 1984–2021 due to longer data gaps in earlier SL records.

scales. Two regions of particularly high coherence are evident: one between 2 and 3 d during summer (JJA), and another on longer time scales (periods exceeding about 6 d) during the colder part of the year (SON and DJF). The strongest coherence occurs at planetary scales during autumn (SON), at periods close to 10 d. This pattern reflects the dominant influence of large-scale atmospheric-pressure variations on SL fluctuations through the inverse barometer effect and basin-wide setup. Seasonal differences at planetary scales are evident, with higher coherence in the colder part of the year, indicating stronger coupling between atmospheric and oceanic variability during these periods. At shorter periods (less than about two days), coherence values decrease, suggesting that smaller-scale processes such as seiches, storm surges, and tides play an increasingly important role in SL variability, while the direct influence of air pressure becomes less significant.

As shown in Fig. 2, coherence between SL and MSLP increases markedly at planetary time scales, underscoring the dominant role of large-scale atmospheric-pressure variability in driving long-period SL fluctuations. To better characterise this relationship, Fig. 3a focuses specifically on these long-period variations, comparing lpSL and lpMSLP. The least-squares linear regression and Pearson correlation coefficient indicate a strong physical link between MSLP and SL variations at these timescales ($R^2 = 0.69$; significantly different from zero at the 99% confidence level). The observed SL response (-1.41 cm/hPa) exceeds the ideal inverse barometer value (-1 cm/hPa), which theoretical studies suggest should apply at these timescales in the Mediterranean (Vilibić et al., 2017 and references therein). It is important to note that TG Bakar is not located near a river mouth; therefore, local density variations are expected to be small. As

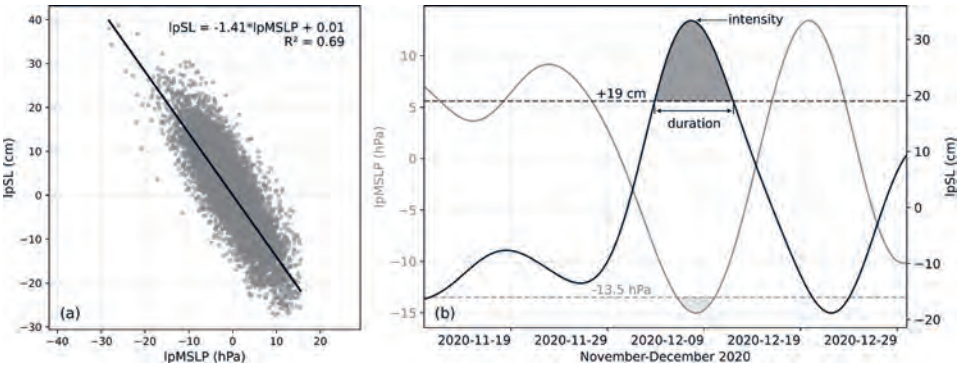


Figure 3. (a) Scatter plot of lpMSLP (ERA5, averaged over the black triangle in Fig. 1) against lpSL at TG Bakar, for 1984–2021 only, due to gaps in earlier SL records. (b) A HIGH-lpSL episode (dark grey shading) and the corresponding LOW-lpMSLP episode (grey shading) during the Adriatic flood of 8 December 2020. Thresholds used to define extreme episodes are shown as dashed horizontal lines.

shown by Pasarić et al. (2000), the enhanced response at these frequencies in the northern Adriatic is largely, though not entirely, explained by wind forcing. At these periods, wind contributes substantial energy and is associated with the same large-scale atmospheric patterns (atmospheric planetary waves). This wind is ageostrophic (in the coastal northern Adriatic region) and acts in the same sense as MSLP changes, thereby amplifying the SL response. The strong correlation between lpSL and lpMSLP at TG Bakar suggests that analysing lpMSLP alone, without accounting for wind, adequately represents the associated lpSL changes.

4. Characteristics of extreme planetary-scale episodes in the current climate

The annual distribution of extremely high episodes of SL on planetary scales (HIGH-lpSL), expressed through their intensity and number, is shown in Fig. 4. The results reveal a clear seasonal pattern, with the highest occurrence and intensity of events during the colder part of the year, while the warmer seasons display fewer and generally weaker episodes. This distribution reflects stronger large-scale atmospheric forcing and more frequent low-pressure systems over the Adriatic during the colder part of the year, consistent with enhanced cyclonic activity in the wider Mediterranean region (Horvath et al., 2008; Flaounas et al., 2022).

It should be emphasized that the distribution of extremely high total SL (i.e. flooding events) follows the presented pattern only toward the end of the year (not shown), coinciding with the Sirocco (southeasterly) wind season in late autumn and early winter. Although lpSL does not reach its largest amplitudes

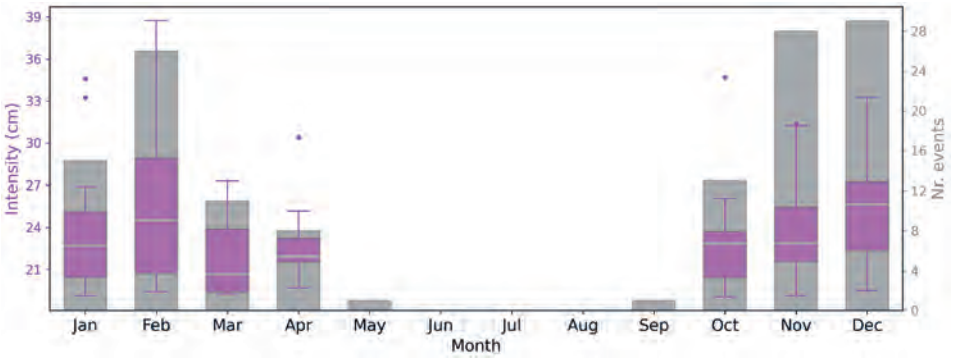


Figure 4. Annual distribution of extreme *planetary-scale component* episodes (HIGH-lpSL): their intensities (magenta boxplots) and number of events (grey bars).

during this period (these occur earlier in the year), it appears most frequently and, combined with the seasonally elevated mean SL (Međugorac et al., 2005; their Fig. A1), creates favorable conditions for flooding in the northern Adriatic. In contrast, while HIGH-lpSL are frequent and strong at the beginning of the year, they coincide with a seasonally lower mean SL, which does not favour the development of flooding events. During this period, however, the large lpSL amplitudes, in their negative phase, act together with the low mean SL to produce extremely low total SL along the eastern Adriatic coast (Šepić et al., 2022).

The long-term evolution of HIGH-lpSL is shown in Fig. 5. The temporal distribution of events shows substantial interannual variability but no pronounced long-term trend in either intensity or duration (trends are not significantly different from zero at the 95% confidence level). The most intense events, exceeding 30 cm, occurred sporadically throughout the record, with somewhat more frequent occurrences after 2010. Episode durations typically range from 3 to 6 d, with occasional events lasting more than 10 d. The frequency of HIGH-lpSL events remains stable (trend not significantly different from zero at the 95% confidence level), with typically 1–2 events per year. This suggests that the occurrence of extreme planetary-scale SL episodes has not changed significantly over the past century at TG Bakar. Whether this conclusion applies to other locations in the Adriatic remains uncertain. At the large temporal scales considered here, the SL response is generally coherent along the basin. For example, Orlić (1983) showed that SL variability at timescales of 10–100 d exhibits a similar temporal evolution over a one-year period at three stations along the Adriatic (Rovinj, Split and Bar). Pasarić et al. (2000) further demonstrated that, although these disturbances are basin-wide, substantial along-basin gradients can occasionally occur: during the most energetic event analysed, differences of 9 hPa in lpMSLP and 17 cm in lpSL were observed between Bakar and Dubrovnik. More recently, Šepić et al. (2022) confirmed that at 10–100 d timescales

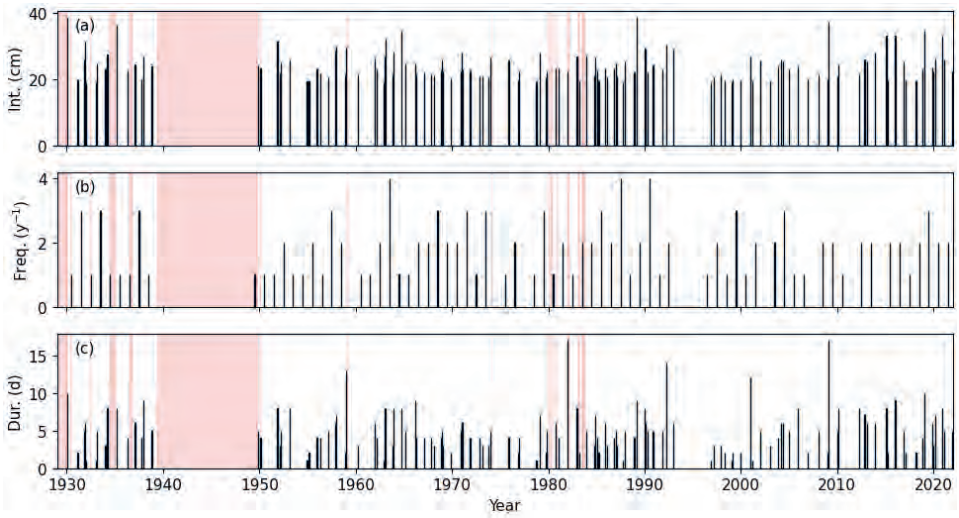


Figure 5. Temporal distribution of extreme *planetary-scale component* episodes (HIGH-lpSL): (a) intensity, expressed as the maximum SL reached during each episode; (b) frequency, expressed as the number of episodes per year; (c) episode duration. Periods with missing SL data are indicated in red.

the Adriatic (from Venice to Dubrovnik) responds in phase, with amplitudes slightly increasing toward the north. Therefore, it is reasonable to hypothesise that our conclusion, based on Bakar SL data, may apply to the entire Adriatic. However, this assumption would need to be confirmed through analysis of additional stations.

5. Evaluation of regional climate models

To assess the skill of RCMs in representing planetary-scale atmospheric forcing, we compared the seasonal cycle, intensity, frequency, and duration of LOW-lpMSLP episodes simulated by three RCMs (ALADIN, CCLM, and RACMO) with ERA5 reanalysis data for the historical period (1971–2000). The RCM simulations were taken from historical experiments in which the RCMs were driven by the GCMs listed in Table 1. Consequently, the evaluated simulations are independent of ERA5, avoiding any potential circularity. The results are summarised in Figs. 6 and 7 using bar and violin plots.

The seasonal distribution of LOW-lpMSLP episodes, as shown in Fig. 6, reveals that all three RCMs reproduced the general seasonal cycle found in ERA5, with a pronounced maximum during the extended winter season (November–March) and minimal activity in summer. However, RCMs tend to overestimate the number of episodes in most winter months, particularly in January and February, with RACMO exhibiting the largest positive bias. The maximum

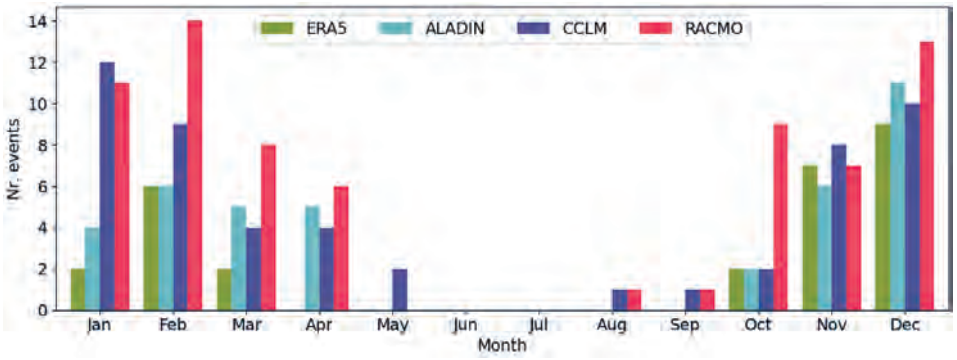


Figure 6. Annual distribution of the number of LOW-lpMSLP episodes, calculated from average MSLP over the northern Adriatic (domain shown in Fig. 1), based on ERA5 (green) and three RCM simulations for the period 1971–2000.

in November and December is well captured by all RCMs, though again with slight overestimation. Spring and autumn episodes were absent or rare in ERA5 and were generally well reproduced by the RCMs. However, CCLM and RACMO simulated a few spurious events in May, August, and September, and all three RCMs generated events in April. Despite some overestimation, particularly by RACMO, the seasonal timing of events was broadly consistent with ERA5. The chi-square test of homogeneity indicated no statistically significant differences in the seasonal distribution of LOW-lpMSLP episodes between ERA5 and the three RCMs, suggesting that the models are suitable for assessing projected changes in seasonal occurrence.

All RCMs broadly captured the distribution of episode intensity (Fig. 7a), with median values (~-15 to -17 hPa) closely aligned with the ERA5 benchmark (~-15 hPa). RACMO exhibited a slightly longer lower tail, indicating a few deep-

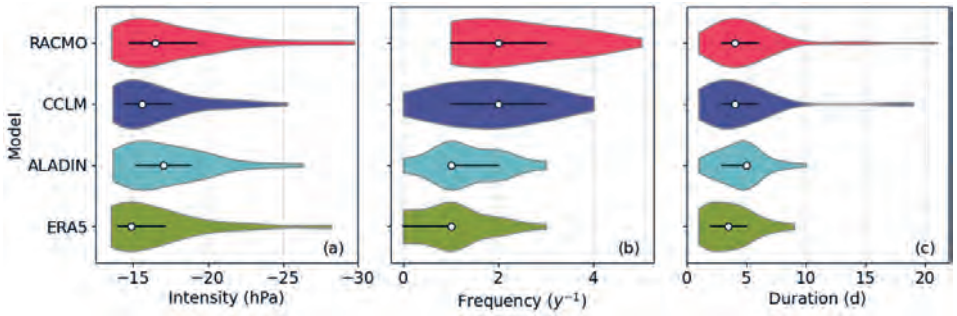


Figure 7. Intensity (a), frequency (b), and duration (c) of LOW-lpMSLP episodes, derived from average MSLP over the northern Adriatic (domain shown in Fig. 1), based on ERA5 and three RCM simulations for the period 1971–2000. Circles denote the median of each distribution, and black lines indicate the interquartile range (25th–75th percentile).

er events than those recorded in ERA5. Nonetheless, the medians and interquartile ranges were generally consistent across datasets, suggesting that the RCMs realistically reproduced the magnitude of extreme low-pressure episodes. Episode frequency (Fig. 7b) showed greater variability among models. ERA5 exhibited a median of approximately one event per year, which was matched by ALADIN. CCLM and RACMO showed higher frequencies (medians close to ~2 events per year), with RACMO simulating up to five events in some years. These differences may reflect how individual models represent the persistence or recurrence of planetary-scale patterns, as well as variations in internal model variability due to parameterisations. The duration of episodes is shown in Fig. 7c. ERA5 exhibited relatively short-lived events, typically lasting 2–5 d. ALADIN produced a very similar distribution, with a slightly higher median (~5 d), while CCLM and RACMO simulated much longer episodes, with upper ranges exceeding 15 d.

Despite some inter-model variability, the evaluated RCMs demonstrated adequate skill in reproducing the key characteristics of LOW-lpMSLP episodes in the historical period. All models realistically captured episode intensity compared to ERA5, with comparable medians and distributions. The Kolmogorov–Smirnov test confirmed agreement for CCLM and RACMO, whereas ALADIN showed a statistically significant difference from ERA5 at the 5% significance level. Frequency and duration exhibited greater inter-model spread, with RACMO overestimating both metrics. For frequency, the Kolmogorov-Smirnov test indicated statistically significant differences between ERA5 and both CCLM and RACMO, while for duration no statistically significant differences were detected. Nonetheless, ERA5 values were encompassed within the model ranges, generally supporting the ensemble's reliability. These results justify the use of the selected RCMs for analysing future changes in planetary-scale low-pressure events, particularly when focusing on relative trends and ensemble-based interpretation.

6. Properties of low pressure events in future climate scenarios

To assess the impact of climate change on the occurrence of extreme atmospheric planetary-scale events, we analysed the projected intensity, frequency, and duration of LOW-lpMSLP episodes over the northern Adriatic for two future periods (2039–2068 and 2069–2098) under RCP4.5 and RCP8.5 scenarios. Results from three RCMs were compared with the historical baseline (1971–2000) (Fig. 8).

No robust trend emerged in event intensity (Fig. 8a). All models exhibited variability across time periods and scenarios, but without a clear or consistent increase or decrease. For most models, median values remained stable between the historical and future periods. While ALADIN and RACMO suggested a modest reduction in the most extreme values (shorter lower tail) under both sce-

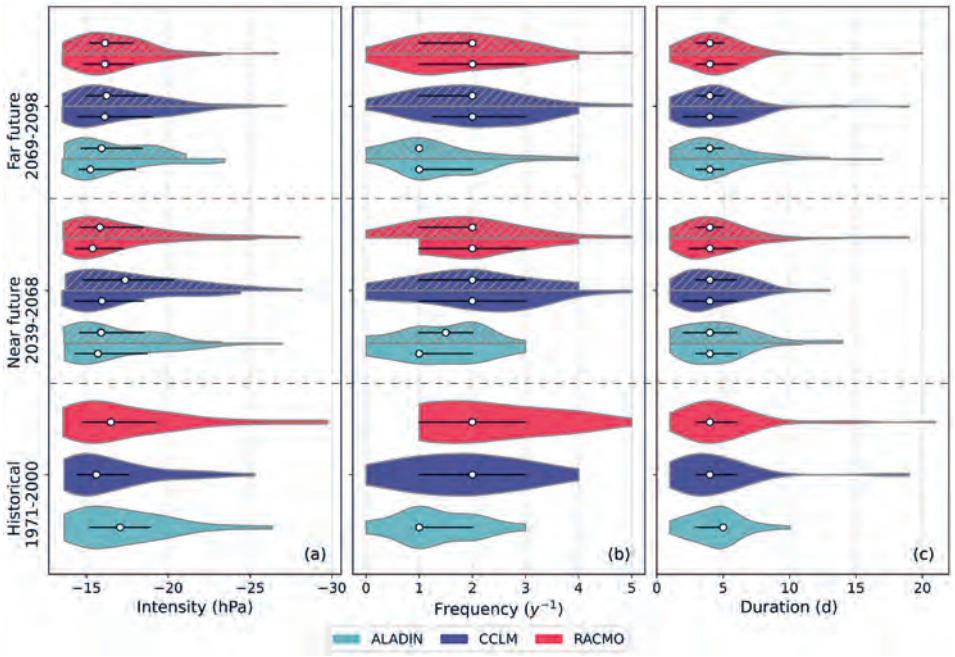


Figure 8. Intensity (a), frequency (b), and duration (c) of LOW-lpMSLP episodes, calculated from averaged MSLP over the northern Adriatic (domain shown in Fig. 1), for three RCMs in the historical period and future periods under RCP4.5 and RCP8.5 (hatched halves of violins) scenarios. Circles denote the median of each distribution, and black lines indicate the interquartile range (25th–75th percentile).

narios and in both future periods, this shift remained within the interquartile range. Overall, model consensus suggests that the intensity of LOW-lpMSLP may not change substantially under future climate conditions.

Projections of episode frequency (Fig. 8b) revealed a wider spread among models. ALADIN showed minimal change under both scenarios and across both future periods. CCLM indicated a modest increase in the upper tail, suggesting a potential rise in the number of events under both scenarios. RACMO projected the most pronounced changes, with the lower tail of its distribution suggesting fewer events per year by 2098 under RCP8.5, despite stable median values. However, the substantial overlap in interquartile ranges with the historical baseline highlights significant internal variability and potential model-specific sensitivities.

The projected duration of LOW-lpMSLP episodes (Fig. 8c) showed only minor changes in median values, with most events remaining in the 2–5 d range. ALADIN exhibited slightly lower medians in both near and far future periods across both scenarios, along with a longer upper tail. CCLM and RACMO tended to simulate similar or shorter durations in the future, with medians remaining

unchanged relative to the historical period. Overall, these results suggest that the duration of LOW-lpMSLP episodes may decrease slightly or remain stable under future climate conditions.

The seasonal distribution (not shown) of LOW-lpMSLP events under future scenarios exhibits a pronounced and persistent modulation in both frequency and intensity across all RCMs. The largest number of events consistently occurs during the cold season (October–April), while events are rare or absent during late spring and summer (May–September). A similar seasonal pattern is evident in event intensity: the strongest amplitudes occur during the cold months, whereas summer events, when present, are generally weaker. This seasonal structure remains largely unchanged between the near and far future periods and under both RCP4.5 and RCP8.5 scenarios. Among the models, CCLM and RACMO generally simulate a higher number of events and somewhat stronger intensities compared to ALADIN, although the overall seasonal pattern is consistent across all three RCMs.

The use of MSLP as a proxy for future SL variability was justified by both physical coherence and practical considerations. First, MSLP and SL variability exhibited strong coherence at time scales 10–100 d (Fig. 2), ensuring that the dominant atmospheric forcing mechanisms can be robustly represented. Second, atmospheric RCM simulations were far more widely available, standardized, and systematically archived than regional ocean or SL-focused climate simulations. Large coordinated initiatives such as EURO-CORDEX (Jacob et al., 2014) and Med-CORDEX (Ruti et al., 2016; Somot et al., 2018) have produced extensive ensembles of atmospheric RCM outputs across multiple models, boundary conditions, and climate scenarios. In contrast, long, scenario-based regional ocean simulations remain limited and inconsistent across modelling groups, and regional SL projections generally rely on downscaling and on combining multiple contributions rather than on fully resolved high-resolution regional ocean climate simulations (e.g., Hermans et al., 2020; Fox-Kemper et al., 2021). Consequently, relying on MSLP allowed the analysis to make use of the limited but methodologically consistent set of available atmospheric RCM projections, which would not have been possible with regional SL simulations.

The ensemble used in this study consisted of three intentionally selected and mutually independent RCM–GCM pairs. This choice ensured that the ensemble captured structural diversity arising from both regional and global model formulations. Furthermore, the selection was constrained to simulations that extended to the end of the 21st century, provided both RCP4.5 and RCP8.5 scenarios, and offered daily MSLP fields, which limited the number of models available at the time. The resulting ensemble was therefore limited in size but met all methodological criteria necessary for a consistent and scenario-complete analysis. Finally, since the climate change signal in the results presented were mostly low, no statistical significance estimates of the projected differences relative to historical climate were provided.

7. Summary and conclusion

This study analyzed planetary-scale (10–100 d) SL variability in the Adriatic Sea using TG Bakar measurements (1929–2021) and MSLP fields from the ERA5 reanalysis and three regional climate model simulations (ALADIN, CCLM, and RACMO). Coherence between air pressure and sea level, as well as the intensity, frequency, and duration of high planetary-scale sea-level episodes, were quantified for the past period. Model performance was evaluated against ERA5, and future changes under the RCP4.5 and RCP8.5 scenarios were assessed to determine whether planetary-scale atmospheric forcing – and its role in coastal flooding – may change in a warmer climate.

The strong coherence between MSLP and SL at periods 10–100 d confirmed that planetary-scale atmospheric pressure dominated *planetary-scale component*, reflected in an enhanced inverse barometer response (-1.41 cm/hPa). The absence of long-term changes in the intensity, frequency, or duration of extreme episodes of *planetary-scale component* suggested climatic stationarity of this process over the twentieth and twenty-first centuries, despite documented global (Gulev et al., 2021) and regional (Lazoglou et al., 2024) warming trends.

In agreement with previous findings of no substantial change in synoptic-scale atmospheric forcing over the Adriatic (Međugorac et al., 2021), our results suggest that planetary-scale forcing will also remain largely unchanged under future RCP scenarios. This represents a novel contribution, as the influence of climate change on planetary-scale processes in the Adriatic Sea has so far received no attention.

The *planetary-scale component* acts as a baseline modulation of sea level, producing prolonged elevated conditions that preconditions major floods when combined with other processes. Since the characteristics of its atmospheric driver are not projected to intensify in the future, the primary driver of increasing coastal flood hazard is expected to be mean sea-level rise rather than enhanced planetary-scale forcing. Basin-averaged Mediterranean SL is projected to increase by ~10–26 cm by mid-century (Galassi and Spada, 2014), while projections for the Adriatic Sea indicate a rise of ~3 mm/y by 2050 (Verri et al., 2024). Nevertheless, even unchanged planetary-scale forcing, superimposed on a rising mean sea level, will increase the probability of compound extreme events.

Because *planetary-scale variability* arises from large-scale circulation regimes, the reliability of its projection is constrained by how well regional climate models and their driving global models reproduce midlatitude Rossby wave dynamics. The regional climate models used in this study reproduced the observed seasonal cycle and event intensity well but showed a moderate spread in duration and frequency, particularly in the RACMO simulation.

Overall, this study suggests that extreme low-pressure anomalies linked to planetary-scale forcing are unlikely to intensify substantially in a warmer climate, at least as represented by the analysed three models.

Acknowledgments – We would like to express our gratitude to the staff of the Geophysical Department (Zagreb) – scientists, technicians, and observers – who have meticulously measured, collected, digitised, and pre-processed sea-level data at TG Bakar. We are also grateful to our colleagues who generously discussed this topic with us and shared their valuable insights. This research has been supported by the Croatian Science Foundation projects IP-2019-04-5875 StVar-Adri and IP-2022-10-4144 CroClimExtremes and by the European Union's Horizon Europe research and innovation program under the Marie Sklodowska-Curie COFUND Postdoctoral Programme grant agreement No.101081355 – SMASH and by the Republic of Slovenia and the European Union from the European Regional Development Fund.

Disclamer – Co-funded by the European Union. Views and opinions expressed are however those of the author(s) only and do not necessarily reflect those of the European Union or European Research Exacutive Agency. Neither the European Union nor the granting authority can be held responsible for them.

Declaration of competing interest – The authors declare that they have no known competing financial interests or personal relationships that could have appeared to influence the work reported in this paper.

References

Cerovečki, I., Orlić, M. and Hendershott, M. C. (1997): Adriatic seiche decay and energy loss to the Mediterranean, *Deep-Sea Res. Pt. I.*, 44, 2007–2029, https://doi.org/10.1016/S0967-0637(97)00056-3.

Ferrarin, C., Bajo, M., Benetazzo, A., Cavaleri, L., Chiggiato, J., Davison, S., Davolio, S., Lionello, P., Orlić, M. and Umgiesser, G. (2021): Local and large-scale controls of the exceptional Venice floods of November 2019, *Prog. Oceanogr.*, 197, 102628, https://doi.org/10.1016/j.pocean.2021.102628.

Ferrarin, C., Lionello, P., Orlić, M., Raicich, F. and Salvador, S. (2022): Venice as a paradigm of coastal flooding under multiple compound drivers, Sci. Rep., 12, 5754, https://doi.org/10.1038/s41598-022-09652-5.

Flaounas, E., Davolio, S., Raveh-Rubin, S., Pantillon, F., Miglietta, M. M., Gaertner, M. A., Hatzaki, M., Homar, V., Khodayar, S., Korres, G. and Kotroni, V. (2022): Mediterranean cyclones: Current knowledge and open questions on dynamics, prediction, climatology and impacts, *Weather. Clim. Dynam.*, 3(1), 173–208, https://doi.org/10.5194/wcd-3-173-2022.

Fox-Kemper, B., Hewitt, H. T., Kuhlbrodt, T., Krasting, J. P., Orr, J. C., Proistosescu, C., Qin, Y., Rao, S., Renwick, J., Rintoul, S. R., Stephenson, K., Treguier, A.-M., van de Wal, R. and Zanna, L. (2021): Ocean, Cryosphere, and Sea Level Change, in: Climate Change 2021: The Physical Science Basis. Contribution of Working Group I to the Sixth Assessment Report of the Intergovernmental Panel on Climate Change, edited by: Masson-Delmotte, V., Zhai, P., Pirani, A., Connors, S. L., Péan, C., Berger, S., et al., Cambridge University Press, Cambridge, 1211–1362 pp., https://doi.org/10.1017/9781009157896.011.

Galassi, G. and Spada, G. (2014): Sea-level rise in the Mediterranean Sea by 2050: roles of terrestrial ice melt, steric effects and glacial isostatic adjustment, Global Planet. Change, 123, 55–66, https://doi.org/10.1016/j.gloplacha.2014.10.007.

Gulev, S. K., Thorne, P. W., Ahn, J., Dentener, F. J., Domingues, C. M., Gerland, S., Gong, D., Kaufman, D. S., Nnamchi, H. C., Quaas, J., Rivera, J. A., Sathyendranath, S., Smith, S. L., Trewin, B., von Schuckmann, K. and Vose, R. S. (2021): Changing State of the Climate System,

in: Climate Change 2021: The Physical Science Basis. Contribution of Working Group I to the Sixth Assessment Report of the Intergovernmental Panel on Climate Change, edited by: Masson-Delmotte, V., Zhai, P., Pirani, A., Connors, S. L., Péan, C., Berger, S., et al., Cambridge University Press, Cambridge, 287–422 pp., https://doi.org/10.1017/9781009157896.004.

Hermans, T. H., Tinker, J., Palmer, M. D., Katsman, C. A., Vermeersen, B. L. and Slangen, A. B. (2020): Improving sea-level projections on the Northwestern European shelf using dynamical downscaling, *Clim. Dyn.*, 54(3), 1987–2011, https://doi.org/10.1007/s00382-019-05104-5.

Hersbach, H., Bell, B., Berrisford, P., Hirahara, S., Horányi, A., Muñoz-Sabater, J., Nicolas, J., Peubey, C., Radu, R., Schepers, D., Simmons, A., Soci, C., Abdalla, S., Abellan, X., Balsamo, G., Bechtold, P., Biavati, G., Bidlot, J., Bonavita, M., De Chiara, G., Dahlgren, P., Dee, D., Diamantakis, M., Dragani, R., Flemming, J., Forbes, R., Fuentes, M., Geer, A., Haimberger, L., Healy, S., Hogan, R. J., Hólm, E., Janisková, M., Keeley, S., Laloyaux, P., Lopez, P., Lupu, C., Radnoti, G., de Rosnay, P., Rozum, I., Vamborg, F., Villaume, S. and Thépaut, J.-N. (2020): The ERA5 global reanalysis, *Q. J. Roy. Meteor. Soc.*, 146, 1999–2049, https://doi.org/10.1002/qj.3803.

Hersbach, H., Bell, B., Berrisford, P., Biavati, G., Horányi, A., Muñoz Sabater, J., Nicolas, J., Peubey, C., Radu, R., Rozum, I., Schepers, D., Simmons, A., Soci, C., Dee, D. and Thépaut, J. N. (2023): ERA5 hourly data on single levels from 1940 to present, Copernicus Climate Change Service (C3S) Climate Data Store (CDS) [dataset], https://doi.org/10.24381/cds.adbb2d47.

Horvath, K., Lin, Y. L. and Ivančan-Picek, B. (2008): Classification of cyclone tracks over the Apennines and the Adriatic Sea, *Mon. Weather Rev.*, 136(6), 2210–2227, https://doi.org/10.1175/2007MWR2231.1.

Jacob, D., Petersen, J., Eggert, B. et al. (2014): EURO-CORDEX: new high-resolution climate change projections for European impact research, *Reg. Environ. Change*, 14, 563–578, https://doi.org/10.1007/s10113-013-0499-2.

Katragkou, E., Sobolowski, S.P., Teichmann, C., Solmon, F., Pavlidis, V., Rechid, D., Hoffmann, P., Fernández, J., Nikulin, G., and Jacob, D., (2024): Delivering an improved framework for the new generation of CMIP6-driven EURO-CORDEX regional climate simulations, *B. Am. Meteorol. Soc.*, 105(6), E962–E974. https://doi.org/10.1175/BAMS-D-23-0131.1.

Lazoglou, G., Papadopoulos-Zachos, A., Georgiades, P., Zittis, G., Velikou, K., Manios, E. M. and Anagnostopoulou, C. (2024): Identification of climate change hotspots in the Mediterranean, *Sci. Rep.*, 14, 29817, https://doi.org/10.1038/s41598-024-80139-1.

Lionello, P., Mufato, R. and Tomasin, A. (2005): Sensitivity of free and forced oscillations of the Adriatic Sea to sea level rise, *Clim. Res.*, 29, 23–39, https://doi.org/10.3354/cr029023.

Marcos, M., Tsimplis, M. N. and Shaw, A. G. P. (2009): Sea level extremes in southern Europe, *J. Geophys. Res.-Oceans*, 114, C01007, https://doi.org/10.1029/2008JC004912.

Međugorac, I., Jambrošić, K., Dolički, D., Kuzmić, J., Šepić, J., Vrkić Seidl, I. and Gašparac, G. (2025): Catalogue of extreme sea levels recorded at tide-gauge station Bakar in the northeastern Adriatic Sea (Mediterranean), *Ocean Sci.*, 21, 2929–3001, https://doi.org/10.5194/os-21-2929-2025.

Međugorac, I., Pasarić, M. and Güttler, I. (2021): Will the wind associated with the Adriatic storm surges change in future climate?, *Theor. Appl. Climatol.*, 143, 1–18, https://doi.org/10.1007/s00704-020-03379-x.

Međugorac, I., Pasarić, M. and Orlić, M. (2022): Long-term measurements at Bakar tide-gauge station (east Adriatic), *Geofizika*, 39, 149–162, https://doi.org/10.15233/gfz.2022.39.8.

Međugorac, I., Pasarić, M. and Orlić, M. (2024): Historical sea-level measurements at Bakar (east Adriatic), SEANOE [dataset], https://doi.org/10.17882/85171.

O'Neill, B. C., Tebaldi, C., van Vuuren, D. P., Eyring, V., Friedlingstein, P., Hurtt, G., Knutti, R., Kriegler, E., Lamarque, J.-F., Lowe, J., Meehl, G. A., Moss, R., Riahi, K., and Sanderson, B. M. (2016): The Scenario Model Intercomparison Project (ScenarioMIP) for CMIP6, *Geosci. Model Dev.*, 9, 3461–3482, https://doi.org/10.5194/gmd-9-3461-2016.

Orlić, M. (1983): On the frictionless influence of planetary atmospheric waves on the Adriatic sea level, *J. Phys. Oceanogr.*, 13, 1301–1306, https://doi.org/10.1175/1520-0485(1983)013<1301:OTFIOP>2.0.CO;2.

Palumbo, A. and Mazzarella, A. (1982): Mean sea level variations and their practical applications, *J. Geophys. Res.*, 87, 4249–4265, https://doi.org/10.1029/JC087iC06p04249.

Pasarić, M. (2000): Variations of sea level in the Adriatic caused by slowly changing air pressure and wind, University of Zagreb, Zagreb, 113 pp. (in Croatian)

Pasarić, M. and Orlić, M. (1992): Response of the Adriatic sea level to the planetary-scale atmospheric forcing. In *Sea level changes: determination and effects*, *Geophys. Monogr. Ser.*, 69 (eds P.L. Woodworth, D.T. Pugh, J.G. DeRonde, R.G. Warrick and J. Hannah), 29–39 pp, AGU, Washington, D.C.

Pasarić, M. and Orlić, M. (2001): Long-term meteorological preconditioning of the North Adriatic coastal floods, *Cont. Shelf Res.*, 21, 263–278, https://doi.org/10.1016/S0278-4343(00)00078-9.

Pasarić, M., Pasarić, Z. and Orlić, M. (2000): Response of the Adriatic sea level to the air pressure and wind forcing at low frequencies (0.01–0.1 cpd), *J. Geophys. Res. Oceans*, 105, 11423–11439, https://doi.org/10.1029/2000JC900023.

Penzar, B., Orlić, M. and Penzar, I. (1980): Sea-level changes in the Adriatic as a consequence of some wave occurrences in the atmosphere, *Thalassia Jugosl.*, 16, 51–77.

Riahi, K., van Vuuren, D. P., Kriegler, E., Edmonds, J., O'Neill, B. C., Fujimori, S., Bauer, N., Calvin, K., Dellink, R., Fricko, O., Lutz, W., Popp, A., Cuaresma, J. C., Samir, K. C., Leimbach, M., Jiang, L., Kram, T., Rao, S., Emmerling, J., Ebi, K., Hasegawa, T., Havlík, P., Humpenöder, F., Da Silva, L. A., Smith, S., Stehfest, E., Bosetti, V., Eom, J., Gernaat, D., Masui, T., Rogelj, J., Strefler, J., Drouet, L., Krey, V., Luderer, G., Harmsen, M., Takahashi, K., Baumstark, L., Doelman, J. C., Kainuma, M., Klimont, Z., Marangoni, G., Lotze-Campen, H., Obersteiner, M., Tabeau, A., and Tavoni, M. (2017): The Shared Socioeconomic Pathways and their energy, land use, and greenhouse gas emissions implications: An overview, *Global Environ. Chang.*, 42, 153–168, https://doi.org/10.1016/j.gloenvcha.2016.05.009.

Rožić, N. (2009): Hrvatski transformacijski model visina, Državna geodetska uprava, Zagreb.

Ruti, P., Somot, S., Giorgi, F., Dubois, C., Flaounas, E., Obermann, A., Dell'Aquila, A., Pisacane, G., Harzallah, A., Lombardi, E., Ahrens, B., Akhtar, N., Alias, A., Arsouze, T., Aznar, R., Bastin, S., Bartholy, J., Béranger, K., Beuvier, J., Bouffies-Cloché, S., Brauch, J., Cabos, W., Calmanti, S., Calvet, J. C., Carillo, A., Conte, D., Coppola, E., Đurđević, V., Drobinski, P., Elizalde-Arellano, A., Gaertner, M., Galàn, P., Gallardo, C., Gualdi, S., Goncalves, M., Jorba, O., Jordà, G., L'Hévéder, B., Lebeaupin-Brossier, C., Li, L., Liguori, G., Lionello, P., Maciàs, D., Nabat, P., Onol, B., Raikovié, B., Ramage, K., Sevault, F., Sannino, G., Struglia, M., Sanna, A., Torma, C. and Vervatis, V. (2016): Med-CORDEX initiative for Mediterranean climate studies, *Bull. Am. Meteorol. Soc.*, 97(7), 1187–1208, https://doi.org/10.1175/BAMS-D-14-00176.1.

SciPy documentation, Version: 1.17.0, January 11, 2026, https://docs.scipy.org/doc/.

Šepić, J., Pasarić, M., Međugorac, I., Vilibić, I., Karlović, M. and Mlinar, M. (2022): Climatology and process-oriented analysis of the Adriatic sea level extremes, *Prog. Oceanogr.*, 209, 102908, https://doi.org/10.1016/j.pocean.2022.102908.

Somot, S., Ruti, P., Ahrens, B., Coppola, E., Jordà, G., Sannino, G. and Solmon, F. (2018): Editorial for the Med-CORDEX special issue, *Clim. Dyn.*, 51, 771–777, https://doi.org/10.1007/s00382-018-4325-x.

Taherkhani, M., Vitousek, S., Bernard, P. L., Frazer, N., Anderson, T. R. and Fletcher, C. H. (2020): Sea-level rise exponentially increases coastal flood frequency, *Sci. Rep.*, 10, 6466, https://doi.org/10.1038/s41598-020-62188-4.

Tsimplis, M. N. and Vlahakis, G. N. (1994): Meteorological forcing and sea level variability in the Aegean Sea, *J. Geophys. Res.*, 99, 9879–9890, https://doi.org/10.1029/94JC00479.

Verri, G., Furnari, L., Gunduz, M., Senatore, A., Santos da Costa, V., De Lorenzis, A, Fedele, G, Manco, I., Mentaschi, L., Clementi, E., Coppini, G., Mercogliano, P., Mendicino, G. and Pinardi, N. (2024): Climate projections of the Adriatic Sea: role of river release, *Front. Clim.,* 6, 1368413, https://doi.org/10.3389/fclim.2024.1368413.

Vilibić, I., Šepić, J., Pasarić, M. and Orlić, M. (2017): The Adriatic Sea: a long-standing laboratory for sea level studies, *Pure Appl. Geophys.,* 174(10), 3765–3811, https://doi.org/10.1007/s00024-017-1625-8.

Vitousek, S., Barnard, P. L., Fletcher, C. H., Frazer, N., Erikson, L. and Storlazzi, C. D. (2017): Doubling of coastal flooding frequency within decades due to sea-level rise, *Sci. Rep.*, 7, 1399, https://doi.org/10.1038/s41598-017-01362-7.

Weisse, R., Bellafiore, D., Menéndez, M., Méndez, F., Nicholls, R. J., Umgiesser, G. and Willems, P. (2014): Changing extreme sea levels along European coasts, *Coast. Eng.*, 87, 4–14, https://doi.org/10.1016/j.coastaleng.2013.10.017.

Welch, P. (1967): The use of the fast Fourier transform for the estimation of power spectra: A method based on time averaging over short, modified periodograms, *IEEE Trans. Audio Electroacoust.*, 15, 70–73, https://doi.org/10.1109/TAU.1967.1161901.

Wilks, D. S. (2019): *Statistical methods in the atmospheric sciences.* Elsevier Inc., Amsterdam, 840 pp. https://doi.org/10.1016/C2017-0-03921-6.

SAŽETAK

Svojstva planetarne komponente vodostaja u Jadranu u sadašnjoj i budućoj klimi

Iva Međugorac i Ivan Güttler

Varijabilnost razine mora na planetarnoj skali (10 – 100 dana) izražen je proces u Jadranskom moru i važan čimbenik koji prethodi obalnim poplavama. U ovom radu okarakterizirali smo njezina svojstva u sadašnjoj klimi koristeći gotovo stoljetni niz mareografskih mjerenja u Bakru (1929. – 2021.) te tlak na srednjoj razini mora iz ERA5 reanalize, a projicirane promjene procijenili smo pomoću triju regionalnih klimatskih modela (ALADIN, CCLM, RACMO). Visoka koherenca između razine mora i tlaka zraka na srednjoj razini mora u pojasu 10 – 100 dana opravdava korištenje atmosferskog tlaka kao zamjene za planetarnu komponentu razine mora u budućoj klimi. Ekstremne epizode na planetarnoj skali definirane su kao odstupanja razine mora ≥ +19 cm (98. percentil razine mora u Bakru filtrirane u rasponu od 10 – 100 dana) i prizemnog tlaka zraka ≤ -13,5 hPa, razdvojene najmanje deset dana. U proteklom razdoblju extremne epizode razine mora dosezale su maksimum u hladnom dijelu godine, javljale se jednom do dva puta godišnje, trajale tri do šest dana i nisu pokazale značajan dugoročni trend intenziteta, učestalosti ili trajanja. Simulacije regionalnih klimatskih modela za razdoblje 1971. – 2000. Pokazale su da svi modeli reproduciraju opaženi sezonski ciklus i intenzitet epizoda, dok su modeli CCLM i osobito RACMO imali tendenciju precjenjivanja učestalosti i trajanja događaja. Projekcije za buduća razdoblja (2039. – 2068. i 2069. – 2098.) prema scenarijima RCP4.5 i RCP8.5 ne ukazuju na postojane promjene u intenzitetu, trajanju ili učestalosti epizoda, što sugerira da se prinudno atmosfersko djelovanje na planetarnoj skali nad sjevernim Jadranom vjerojatno neće znatnije promijeniti u toplijoj klimi. Posljedično, budući rizik od poplava bit će prvenstveno određen

porastom srednje razine mora te superpozicijom procesa na različitim vremenskim skalama, a ne o jačanju planetarnih procesa.

Ključne riječi: Jadransko more, razina mora, tlak zraka na srednjoj razini mora, planetarna komponenta razine mora, regionalni klimatski modeli, RCP4.5, RCP8.5

Corresponding author's address: Iva Međugorac, University of Nova Gorica, Vipavska 13, SI-5000 Nova Gorica, Slovenia. iva.medugorac@ung.si

This work is licensed under a Creative Commons Attribution-NonCommercial 4.0 International License.